

Compensating for ultrasound frequency attenuation in tissue when determining effective particle size

Karolina Sandell

2021

Master's Thesis in
Biomedical Engineering

Supervisor: Tobias Erlöv

Lund University
Faculty of Engineering LTH
Department of Biomedical Engineering

Abstract

Giant cell arteritis is a disease that affects the arteries, for example the temporal artery. When affecting the temporal artery, it can cause serious consequences such as blindness and stroke. The existing methods for diagnosing the disease are invasive, time consuming and costly. Ultrasound would therefore be an attractive diagnostic alternative providing a lot of benefits. Information about the characteristics of tissue can be obtained from the frequency spectra of the ultrasound echo pulse. This can be used to distinguish diseased tissue from healthy tissue.

When using this method in *in vivo* studies, the tissue, for example the skin, between the ultrasound transducer and the tissue being investigated also impacts the frequency spectra of the ultrasound pulse. This project examines this impact and how to compensate for it so that it does not influence the measurements of the actual tissue being investigated. A graphical user interface is also developed as a tool for evaluating measurement data obtained during the *in vivo* study.

It was found that the frequency attenuation in the tissue between the skin and the tissue being investigated can be approximated as linear. When compensating for this attenuation it is not possible to use a general compensation curve for all patients. The compensation has to be done individually for each patient.

Table of contents

Table of Contents

Abstract.....	i
Table of contents.....	ii
1. Introduction	1
1.1 Background.....	1
1.2 Aim	2
2. Theory	3
2.1 Ultrasound.....	3
2.2 Center frequency shift (CFS)	6
2.2.1 Pulse center frequency and particle size	6
2.2.2 Successful application.....	10
2.3 Giant cell arteritis (GCA)	11
3. Method.....	13
3.1 Ultrasound data.....	13
3.2 Data conversion.....	14
3.3 Frequency attenuation between skin and artery	16
3.4 Finding the skin	17
3.5 Removing the outliers	18
3.6 Shifting the B-mode image	20
3.7 Shifting the frequency matrix.....	23
3.8 Measurements on phantoms	23
3.9 GUI	24
4. Results.....	26
4.1 Horizontalizing the skin	26
4.2 Shifting the frequency matrix.....	29
4.3 Measurements on phantoms	30
4.4 Calculating the attenuation	33

5. Discussion.....	35
5.1 Horizontalizing the skin	35
5.2 Measurements on phantoms	36
5.3 Calculating the frequency attenuation	37
6. Conclusion	38
7. References.....	39

1. Introduction

1.1 Background

Ultrasound is a non-invasive way of studying internal organs. An ultrasound transducer is used to send ultrasound pulses into the body and receive the returning ultrasound echoes. In this thesis high frequency ultrasound is used to characterize tissue. This is possible since different types of tissue reflects ultrasound differently.

An area where this has been found useful is to determine the risk of an arterial plaque rupturing. More vulnerable plaques have a different composition from less vulnerable plaques and therefore reflect the ultrasound differently [1]. Given the results from that study, it is hypothesized that the technique would also be useful when diagnosing giant cell arteritis (GCA). GCA is a disease that causes inflammation of blood vessels. When this disease affects the temporal artery, it can lead to for example blindness [2] and stroke [3].

When *ex vivo* measurements are made, the ultrasound transducer can be placed in direct proximity of the tissue of interest. But when *in vivo* measurements are performed there is always some additional tissue, for example skin, between the transducer and the tissue being investigated. This additional tissue will have an impact on the ultrasound echoes returning to the tissue of interest, and these changes in the echo need to be compensated for.

This thesis is part of a study (collaboration between the Department of Biomedical Engineering and the Department of Clinical Sciences, Ophthalmology, Lund) aiming to use the frequency content in the ultrasound pulses to diagnose GCA *in vivo*. More specifically, the work within this thesis focuses on the so-called frequency attenuation occurring in the tissue prior to the temporal artery.

1.2 Aim

The main goal of the thesis is to determine the frequency attenuation in the tissue between the skin and the temporal artery using high frequency ultrasound and to determine if there is a general curve describing the frequency attenuation as a function of the depth in the tissue. If such general curve exists it could then be used for every patient to compensate for the attenuation in the tissue prior to the temporal artery. It should be investigated whether the attenuation is dependent on the ultrasound transducer and its settings and if the attenuation can be approximated as linear.

2. Theory

2.1 Ultrasound

Ultrasound is an imaging technique that uses sound of very high frequency to create an image. Frequencies used in diagnosis are commonly in the range of 2-15 MHz, but frequencies as high as 40 MHz are occasionally used. An ultrasound transducer is used to create ultrasound pulses that travels through the tissue. The ultrasound pulse is scattered by cells and small structures within the tissue and the returning echoes are detected by the transducer. [4]

Echoes often have strongest intensity at boundaries where there is a change in the tissue through which the sound travels. The sound is also scattered from small irregularities within tissue. A B-mode image is a cross sectional image visualizing boundaries between different types of tissue, for example different organs. Normally ultrasound images are in grayscale where lighter regions have stronger intensity echoes and darker regions have lower intensity echoes. In this thesis the ultrasound images are in colour for visibility reasons. The colour scale is from yellow to blue instead of white to black. An example of such an image can be seen in Figure 1. Brighter yellow represents regions with stronger intensity echoes and darker blue regions with lower intensity echoes. Disease can be discovered by looking for abnormal anatomical boundaries and changes in how the sound is scattered throughout the tissue [4].

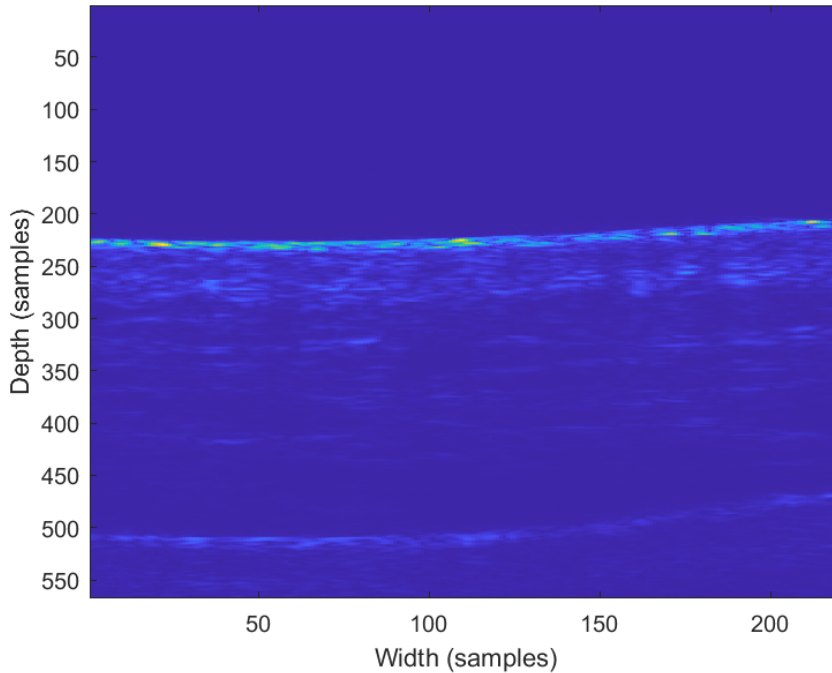


Figure 1. B-mode image of the first frame of patient 1.

The sound from the ultrasound transducer is directed into a narrow beam and short pulses of sound are transmitted into the tissue. One pulse-echo sequence results in one line in the B-mode image. The beam then moves to a new direction and creates the next line and so on. An image can be made up of hundred or more lines. The ultrasound transducer is commonly made up of many small transducer elements placed in a linear array [4]. This can be seen in Figure 2.

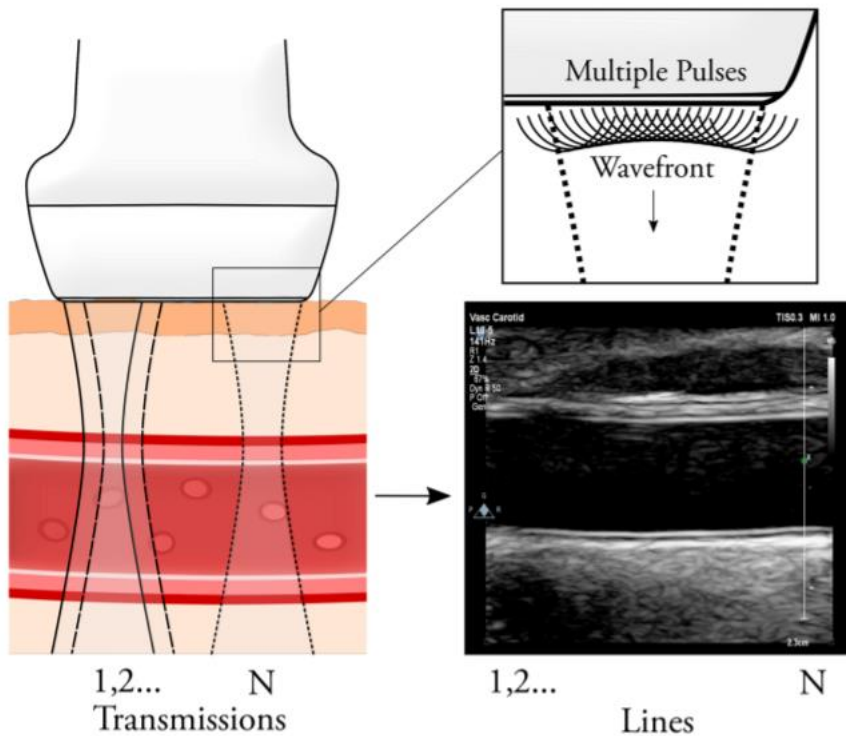


Figure 2. The left side of the image shows the sound from the ultrasound transducer directed into a narrow beam and being transmitted through tissue. The top right corner of the image shows the linear array ultrasound transducer consisting of an array of elements each sending a pulse. The bottom right corner shows a typical grayscale ultrasound image [5].

When the echoes reach the ultrasound transducer calculations are performed to determine the origin of each echo. The time from the pulse was transmitted to the echo is being detected is proportional to the distance of the target from the transducer. The first echoes being detected comes from targets closer to the transducer. The place of the target is in the direction of the pulse [4].

2.2 Center frequency shift (CFS)

2.2.1 Pulse center frequency and particle size

Tissue is made up of different sized particles, where a particle from an acoustic perspective could be individual cells, a group of cells or other structures. Determining the size of the particles can be a way of characterizing the tissue. This can be done with the use of ultrasound by studying the way the sound is scattered by the particles. The measured particle size is not the sizes of all the differently sized particles, but rather an effective acoustic size [6, 7].

The way the sound is scattered by the ultrasound scattering particles is dependent on the effective scatterer radius r and on the wavelength λ of the ultrasound. This is described by the parameter ka .

$$ka = \frac{2\pi}{\lambda} r$$

Figure 3 shows the normalized amplitude of the scattered sound in different directions depending on the parameter ka . It has been shown that when estimating the scatterer size, the optimal range of the parameter ka is $0.5 < ka < 1.2$ [8].

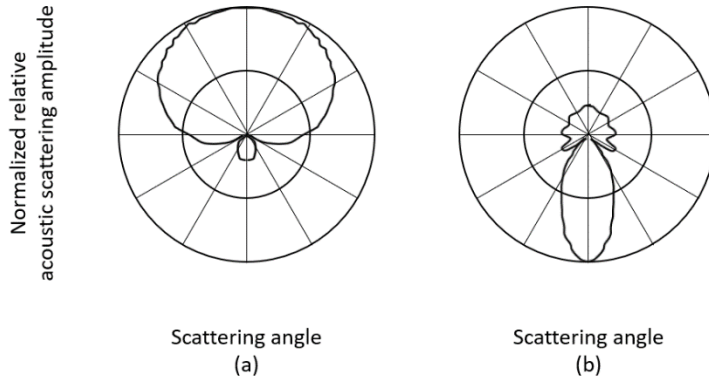


Figure 3. Polar coordinate profile of particle scattering (a) Smaller ka , (b) Larger ka . The ultrasound transducer is placed at the top of the image.

Researchers at the Department of Biomedical Engineering, Faculty of Engineering, Lund University, have studied this relation between scattered ultrasound and particle size [8]. The change in the backscattered sound that they are looking at are the changes in center frequency. The frequency spectrum of the ultrasound pulse is assumed to have a Gaussian shape with a certain center frequency [8]. The scattered sound will also have a Gaussian shaped frequency spectrum, but with a lower center frequency, see Figure 4 [8]. This is because the higher frequencies will be reflected to a lesser extent than the lower, resulting in the backscattered sound having a Gaussian shape peaking at a lower center frequency. Larger particles will reflect a lower center frequency than smaller particles.

The center frequency shift (CFS) is the center frequency compared to the center frequency of the ultrasound signal in a material with very small particles. CFS can be used to estimate the particle size with equation 1.

$$particle\ radius = \sqrt{\frac{CFS}{2 \cdot 0.827 \cdot \sigma^2 \cdot \left(\frac{2\pi}{c}\right)^2}} \quad (1)$$

where c is the speed of sound and σ^2 relates to the pulse bandwidth [8].

Using the reference frequency (F_R), i.e. the frequency backscattered from very small scatterers, the CFS is calculated with equation 2 [8].

$$CFS = \frac{F_R}{CF} - 1 \quad (2)$$

Since the CFS can be used to estimate the size of the scattering particles it can be used to objectively characterize tissue.

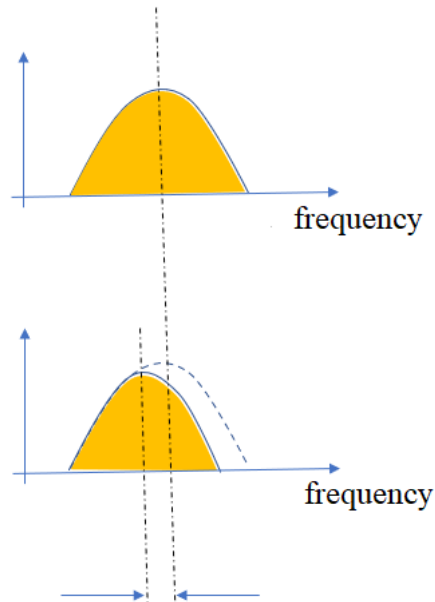


Figure 4. Arrows pointing out the center frequency shift (CFS). The upper image is the spectrum from very small scatterers compared to the wavelength of the ultrasound (reference spectrum) and the lower image is the spectrum from larger scatterers.

However, as the sound travels through the tissue, it will be attenuated. Higher frequencies are attenuated more than lower frequencies. This frequency attenuation causes the center frequency to be depth dependent, even if the particle size stays constant.

Figure 5 illustrates this problem. Imagine that the ultrasound pulse propagates through two homogenous tissues composed of different particle sizes. The first tissue has larger particles than the second and will show a lower center frequency. However, due to the frequency attenuation the center frequency is constantly changing, giving the impression that the particle size changes continuously.

When studying tissue where there is some other tissue between the ultrasound transducer and the tissue being studied, this frequency attenuation needs to be compensated for so that the change in center frequency caused by the tissue being studied is not depth dependent.

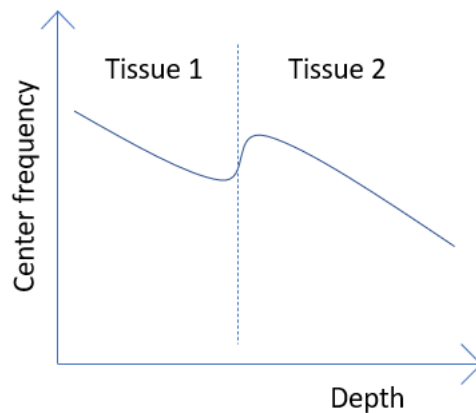


Figure 5. Image visualizing the continuous frequency attenuation and the change in center frequency when the ultrasound enters another type of tissue.

2.2.2 Successful application

CFS as a mean of characterizing tissue has been successfully shown on arterial plaques. An arterial plaque results from a gradual build-up of inflammatory cells in the arterial wall. Plaques can rupture and cause acute cardiovascular events [1].

The risk of a plaque rupturing, its vulnerability, is determined by the content of the plaque. More rupture prone plaque has a core of necrotic debris and lipids, an accumulation of inflammatory cells and a reduced content of fibrous tissue and smooth muscle cells and they are often covered by a thin fibrous cap [1].

Being able to determine the vulnerability of a plaque and treating it before it ruptures is a challenge. Many different imaging techniques, both invasive and non-invasive, such as intravascular imaging, CT, MR and PET/SPECT have been suggested in identification of plaque features, however the use of such techniques is limited due to invasiveness, ionizing radiation, or time requirements [1].

Using ultrasound in plaque identification would be non-invasive, easily tolerable, cost and time effective, give real time results and use no ionizing radiation. Therefore, using CFS would seem like an attractive choice [1].

The CFS method has been evaluated both *ex vivo* and *in vivo*. In the *ex vivo* study a more negative CFS correlated with lipid-richness, more macrophages and haemorrhages and less smooth muscle cells. In the *in vivo* study significant correlations were observed between CFS and collagen and CFS and smooth muscle cells. The CFS correlated inversely with macrophages and the core size of the plaque. No significant correlation was seen between CFS and haemorrhage or CFS and lipids. It should however be noted that the aim is to detect the overall vulnerability and not necessarily individual components of the plaque [1].

The method was then used to determine vulnerability of plaques in *in vivo* pre-operative patients. The outcomes showed that the method has potential to identify vulnerable plaques and prevent acute events [1].

2.3 Giant cell arteritis (GCA)

In this project ultrasound images of patients suspected of having giant cell arteritis (GCA) were investigated. GCA is a disease that causes inflammation of larger blood vessels. The causes are unknown but might be an autoimmune disease. The disease typically affects older Caucasian women [2].

GCA can affect blood vessels in many parts of the body, for example the temporal artery. Temporal artery supplies blood to the head and brain, see Figure 6. The disease causes a narrowing of the artery resulting in symptoms such as headaches, dizziness, and problems with vision. If left untreated GCA of the temporal artery can cause blindness [2], aneurysm and stroke [3].

When a patient has symptoms of GCA of the temporal artery a physical examination is first performed. A biopsy is performed if the symptoms of the patient and the physical examination raises the suspicion that the patient might be suffering from GCA. During the biopsy, a part of the temporal artery is surgically removed [2].

Finding a way to diagnose GCA non-invasively would provide a lot of benefits. Using ultrasound and CFS would be a time and cost-effective alternative that would also be less harmful to the patient.

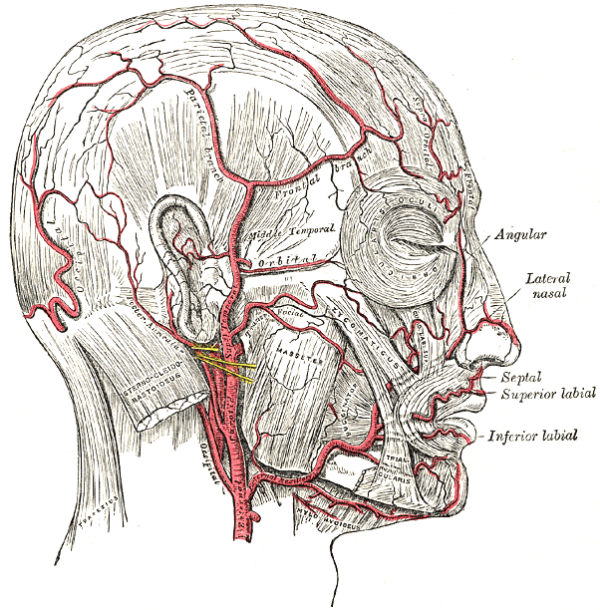


Figure 6. The temporal artery [9].

3.1 Ultrasound data

The data used in this project was *in vivo* high-frequency ultrasound images of the temporal artery in 68 patients, which had already been collected. These patients were suspected GCA positive and was, as part of ongoing research, examined with both ultrasound and photoacoustics at the Department of Clinical Sciences, Ophthalmology, Lund. The scanner used was a Vevo 3100 (FUJIFILM VisualSonics Inc., Toronto, ON, Canada) equipped with a 30 MHz center frequency transducer. The transducer was placed in a holder driven by a stepping motor. Cross sectional scans of the temporal artery were made with step sizes of 0.5 mm. The saved data included both B-mode and Color Doppler measurements.

The same measurements setup, described in [10] was used for both the ultrasound and photoacoustic measurement. This meant that all images were acquired using a laser fiber holder together with a 12 mm gelpad between the transducer and the skin. The gelpad was held in place with plastic wrap. Note that in this project it was only the ultrasound images that were used, not the photoacoustic images. Using this measurement setup, the gelpad gives a relatively large dark area in the top part of the obtained images. Further, the plastic wrap is sometimes visible as a line just above the skin surface. The measurement setup can be seen in Figure 7.

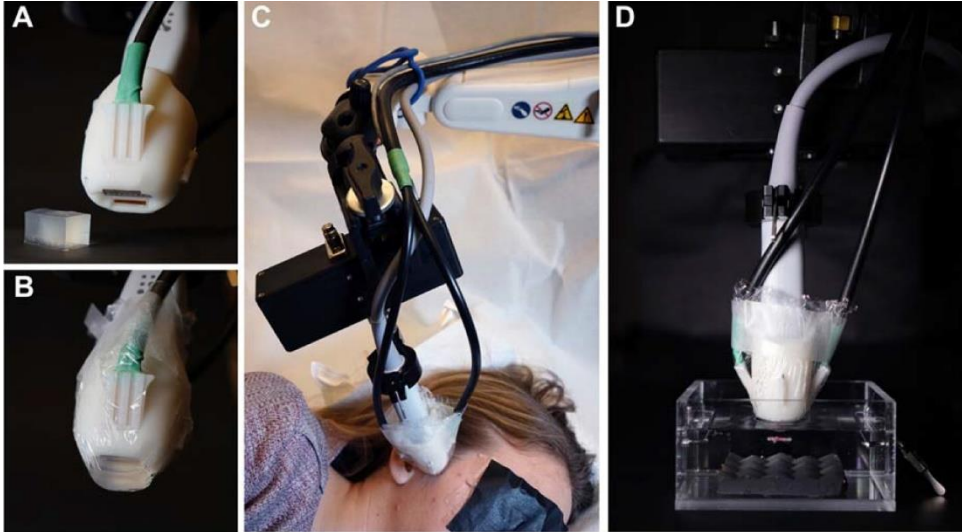


Figure 7. Photographs of the *in vivo* and *ex vivo* examination setups. (a) Close-up view of the transducer before the gel pad is installed and (b) after the gel pad is mounted with plastic wrap. (c) PAI assembly fixed to an adjustable arm with the stepping motor used for *in vivo* measurements, shown examining the temple region of a subject. (d) *Ex vivo* setup showing a section of a temporal artery submerged in water. © 2019 IEEE

3.2 Data conversion

The first task was to use a previously developed MATLAB script to transform the ultrasound data into matrices that could then be used for calculations and images. For each patient three matrices, totA, totB and totC were constructed. The data file of one patient turned out to be faulty and matrices could not be constructed for that patient, resulting in data from 67 patients being used in this project. Matrix totA contains the B-mode ultrasound image amplitude information. Matrix totB and totC contains the center frequency for each pixel in the B-mode and Color Doppler images, respectively. The difference between totB and totC is that different pulse lengths were used. For totB a shorter pulse length was used, which results in a wider frequency spectrum and larger center frequency shifts. For totC a longer pulse length was used, so the frequency spectrum was narrower and

the changes in center frequency that could be detected were much smaller. This is achieved by using the Color Doppler setting for the measurements in totC. Note that the Color Doppler setting was only used because of its longer pulse length and not to acquire actual flow measurements.

A sliding average was used to remove some noise when constructing totB and totC, however care was taken not to deform the frequency curve. The average was chosen to be taken over 11 consecutive values because this created a smoother curve without compromising the shape of the curve, see Figure 8.

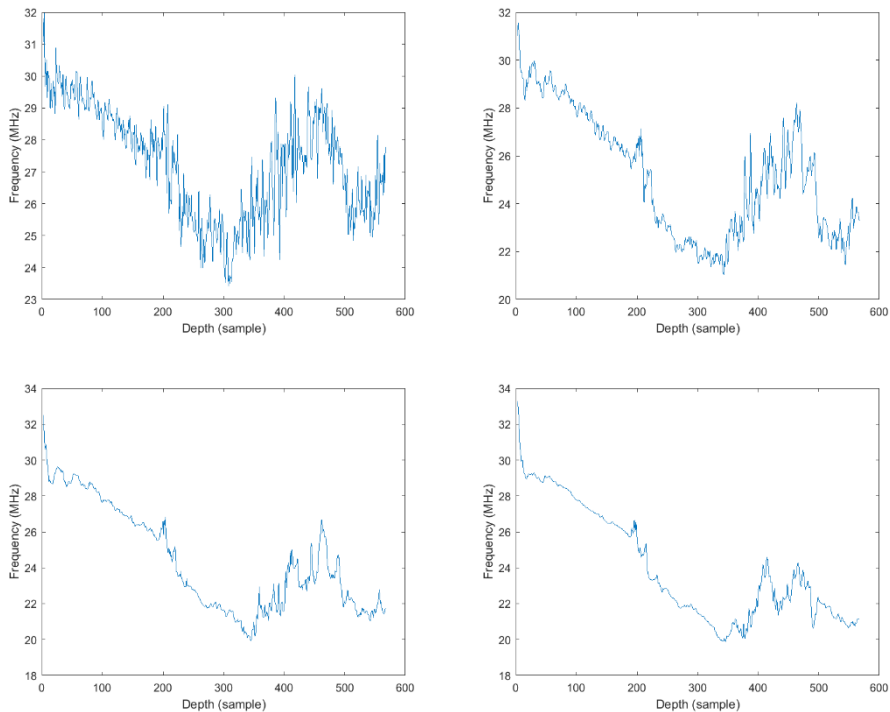


Figure 8. Frequency plot (totB) for frame 1 of patient 1 using different sliding averages when construction the matrix. The averages are taken over none, 5, 11 and 20 values respectively from top left to bottom right image.

For each patient there existed a number of B-mode frames created using the stepper motor. The ultrasound transducer is moved 0.5 mm between each

frame. Different patients' matrices have different number of rows and columns.

The images depicted the gelpad, sometimes the plastic wrap, the skin, the tissue between the skin and the artery and the temporal artery either along the artery or as a cross section of the artery. The skin is more or less horizontal in the image, see Figure 1.

3.3 Frequency attenuation between skin and artery

The main goal of this project is to determine the frequency attenuation in the tissue between the skin and the temporal artery and to find a general curve describing the frequency attenuation as a function of the depth in the tissue. The general curve should then be used for every patient to compensate for the attenuation in the tissue prior to the temporal artery.

Each column in each frame for each patient can be used to plot a curve of how the attenuation changes with the depth. In the plots of the frequency attenuation all columns of all frames from each patient were averaged to create an average frequency attenuation curve for each patient. This resulted in 67 curves. Then an average of all the patients' frequency curves were calculated and their standard deviation.

In order to achieve this, the above-mentioned curves must start at the skin surface for all columns. Since the skin surface might not be horizontally aligned in the image, the following steps were taken. First the skin needs to be identified in the image. This might result in some outliers that are not actually a part of the skin. Then the matrices need to be shifted to create a horizontal skin. These steps are explained in the following sections.

3.4 Finding the skin

The first step is to create an algorithm that can automatically identify the skin in an ultrasound image. This algorithm will first be used to shift the totA-matrix since shifting the B-mode image visualizes whether the skin has been horizontalized or not. But the actual application of the finished algorithm is to shift the totB- and totC-matrix.

The typical appearance of the ultrasound images used in this project is a large dark region at the top followed by a distinct bright line or narrow bright band ending with a large region with a mix of darker and brighter areas, see Figure 9. The top region is the gelpad that was placed between the ultrasound transducer and the skin. The sudden change in brightness marks the skin and the start of the tissue. The large more or less patchy region at the bottom of the image contains a lot of noise. This is because the sound does not have sufficient energy to reach these depths, so there is no ultrasound echo returning to the transducer and hence only noise can be seen.

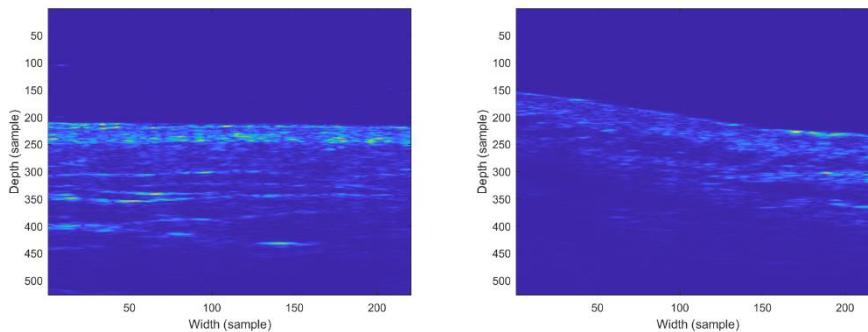


Figure 9. Examples of typical ultrasound images used in this project. The line of the skin can be quite horizontal across the image as seen in the left image, or have some curvature as seen in the right image. The left image is the first frame of patient 1 and the right image is the first frame of patient 89.

First the B-mode image data was convolved with a kernel.

$$kernel1 = [1,1,1,1,1, -1, -1, -1, -1, -1]$$

The kernel was chosen to start with positive values and end with negative values to create a maximum brightness along the skin. With such kernel the positive and negative part will cancel in the gel part of the image. The positive part will then reach the tissue first and create a larger positive than negative part because of the stronger intensity in the tissue. When the negative part then reaches the tissue as well, the positive and negative part will cancel each other again.

A couple of other kernels were also explored, for example a kernel with a heavier center value and also a wider kernel with more than one column, such as below.

$$kernel2 = [ones(5,1); 5; -ones(5,1)]$$

$$kernel3 = [ones(5,10); -ones(5,10)]$$

$$kernel4 = [ones(5,10); 5 * ones(1,10); -ones(5,10)]$$

After convolving the image with the kernel, the maximum intensity of each column was found in the resulting image.

3.5 Removing the outliers

Detecting the skin did quite often result in outliers. The outliers can be single or occur many in a row. The outliers were removed in the following fashion.

When detecting the skin, the output is a vector containing the index of the pixel with the maximum intensity in that column. Figure 10 shows two examples of such output vectors from the program that detects the skin. The peaks are clearly caused by outliers and are not actually a part of the skin.

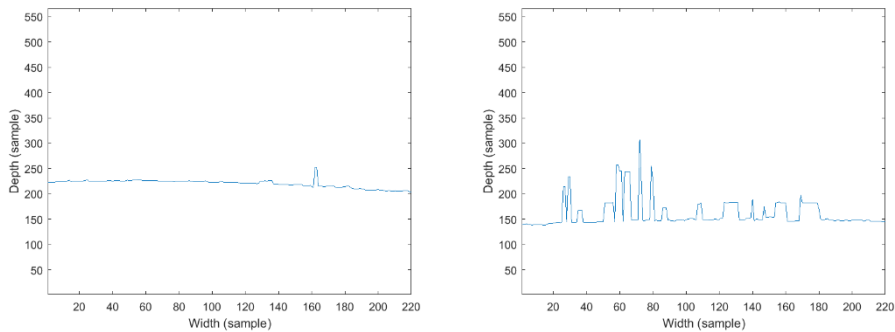


Figure 10. Left: Plot of the output vector from the program that detects the skin (patient 1). Peak caused by outliers. Right: Plot of the output vector from the program that detects the skin (patient 39). Example of two intervals of outliers following each other can be seen in the rightmost part of the image where there is a peak followed by a longer interval of outliers that are clearly not a part of the skin. Observe that the frequency plots are upside down compared to the B-mode images, so the outliers seen in these images are within the tissue and not in the gelpad.

The code for removing the outliers first loops through the vector and compares the adjacent values. When a too large discrepancy between two adjacent values is found it is registered.

This results in the vector being divided into intervals. The longest interval is then assumed to be the skin. In the left image of Figure 10 there would be three intervals and one furthest to the left is assumed to be skin.

The program then continues to first loop through the intervals to the left of the longest interval and then the intervals to the right of it, starting with the interval closest to the longest interval in both cases. Since the longest interval is assumed to be skin the next interval is assumed to be outliers. When moving on to the next interval there are two possibilities. It could be an interval of skin, or it could be another interval of outliers that just differs enough in height from the outliers in the previous interval, see example of this steplike appearance in the right image of Figure 10.

To determine if it is an interval of skin or another interval of outliers, the current interval is compared with the last previous interval of skin that has

been found. This might be the longest interval or a later interval of skin if that has been found.

If an interval is skin, then the following interval always must be outliers, but if an interval is outliers the next interval could be outliers or skin and needs to be compared to the closest previous interval of skin.

When comparing the current interval with an interval of skin, the value of the current interval and the value of the interval of skin closest together are compared to each other. This is because the skin sometimes has a curvature and comparing skin index of points far apart might result in the faulty belief that they do not both belong to the skin.

When it is determined which intervals are outliers and which are skin the outliers are replaced with a linear regression between the two points of skin surrounding the outlier interval.

3.6 Shifting the B-mode image

Now that the skin has been detected, the next step is to shift the columns of the B-mode image to create a horizontal, linear skin surface in all images. An algorithm was created to do this.

The algorithm loops through all the columns in the matrix the columns are shifted to each other so that all pixels containing skin is on the same row as the skin in the first column. When shifting one column in relation to the previous one, this will not result in a square matrix. To create a square matrix NaN values are added in the empty places.

Two values are used when constructing the matrix. These values are a and b , see top left image in Figure 11. The value a is the number of pixels of the previous column that is above the start of the current column. The value b is the number of pixels of the previous column that is below the end of the current column. The value a is positive if the previous column starts above the current and the value b is positive if the previous column ends after the current. It is not necessary so that $a = -b$, except when the second column is

shifted from the first. After adding *NaN* values, the length of the previous and current columns are not equal anymore and it might not be that $a = -b$.

$$a = \text{index}(i - 1) - \text{index}(i)$$

$$b = \text{length}(\text{previous column}) - \text{length}(\text{current column}) + \text{index}(i) - \text{index}(i - 1)$$

When looping through the columns and creating the new, shifted matrix, three scenarios can occur as depicted in Figure 11. One is that $a > 0$ and $b < 0$, one is that $a < 0$ and $b > 0$ and one is that $a \geq 0$ and $b \geq 0$. The last scenario where $a \geq 0$ and $b \geq 0$ can occur whenever the previous column has *NaN* values added either in the beginning, end or both so it is longer than the current column.

After creating the shifted matrix all rows above the row of the skin are removed so that the skin is in the top row of the matrix. At some depth, the rows will start to contain *NaN* values. All rows containing *NaN* values are identified by summing all the values along the row and then removing the row and all the rows below it if the sum is *NaN*.

The resulting shifted B-mode images were used to visually identify if the automatic skin detection and shifting worked satisfactory. When shifting the B-mode images the part of the matrix above the skin was not removed. This was done to clearly see if the skin was horizontalized properly.

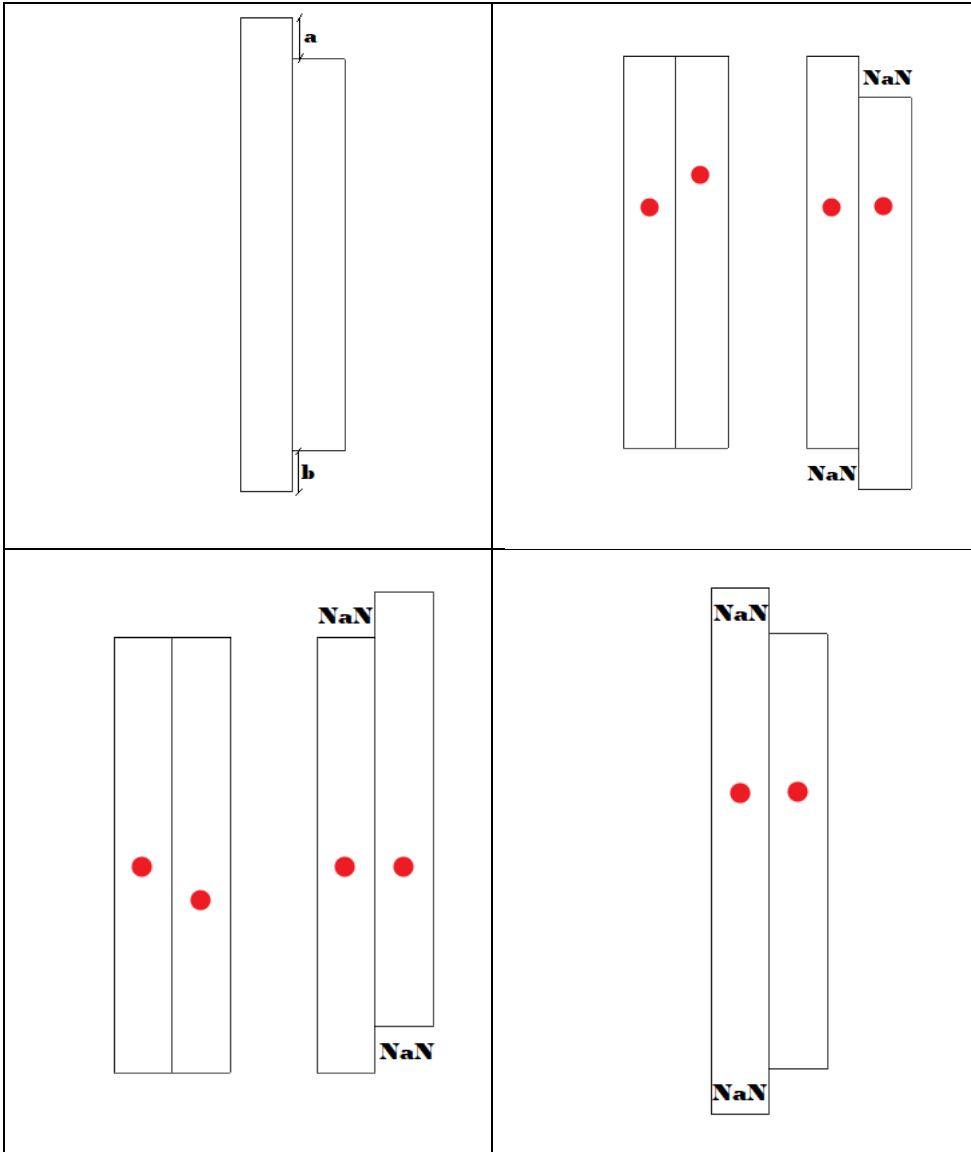


Figure 11. Top left image shows the definition of a and b in the code for shifting matrices. The three other images show the three possible relationships between the previous and the current column. Top right: $a > 0$ and $b < 0$. Bottom left: $a < 0$ and $b > 0$. Bottom right: $a \geq 0$ and $b \geq 0$.

3.7 Shifting the frequency matrix

After shifting the B-mode image to control that the shifting of the matrices worked, the matrices containing frequency data were shifted. Those patients where the shifting of the matrix did not result in horizontal skin were excluded at this point.

When shifting the B-mode images the whole B-mode image was plotted including the large region of the gelpad in the upper part of the image. When shifting the frequency matrix, the part above the horizontal skin was omitted so that all the frequency plots had the skin at the top of the image where the depth is zero. By doing this the tissue at a certain depth will always be at the same row in the matrix and at the same depth in the image.

When plotting the frequency curve of a patient all columns of all frames were averaged to create a plot of the average frequency shift versus the depth.

3.8 Measurements on phantoms

To investigate whether characteristics in the frequency attenuation curves relate to properties of the investigated tissue or to the ultrasound beam profile, measurements were made on phantoms mimicking homogenous tissue.

Three different phantoms were used during these measurements. One was a commercial phantom (Model 047, CIRS Inc. Norfolk, VA, USA). The other two were made at the department from ballistic gel and glass beads. The glass beads have an average diameter of 16 μm and 49 μm respectively. The choice of these phantoms was just a combination of having different materials to investigate, both in terms of background material and size of particles.

The measurements were made with the same setup as for the measurements on patients, with the same transducer, gelpad and plastic wrap. One

exception from the setup was that in the phantom measurements, the transducer was held manually during the acquisition.

Two measurements were made on each phantom. Each measurement contained a different number of frames. The resulting frequency attenuation curves were compared to the ones from the patients.

3.9 GUI

The project also included the development of a graphical user interface (GUI), see Figure 12. It was created as a tool to help clinicians with analysing the center frequency measurements and compensating for the frequency attenuation. This is a necessary step in order to evaluate the acquired *in vivo* data.

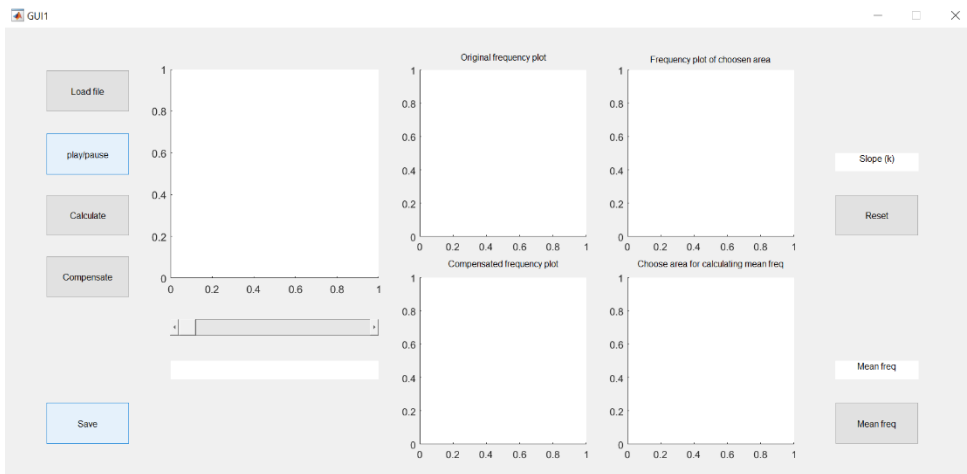


Figure 12. GUI

The GUI loads a .mat-file chosen by the user. The .mat-file should contain the three data matrices totA, totB and totC of a patient. The user can play and pause a slide show of the different B-mode frames of that patient.

A rectangle can be drawn in the B-mode frame. This rectangle is the area in which the attenuation should be calculated. When the calculate button is pressed, the frequency plot of the currently displayed B-mode frame is shown in a figure. The partial frequency plot of the area within the drawn rectangle is shown in another figure. A linear regression is added to the partial frequency plot and its slope is displayed beside the figure.

The user can now decide to change the slope by drawing a new line in the partial frequency plot by clicking at the two points between which the new line should be drawn. The new slope will be displayed beside the figure. If the user would like to return to the original linear regression and slope, the reset button can be pushed.

When the user is satisfied with the slope, the compensation of the frequency attenuation can be done by clicking the compensate button. The complete frequency plot is then compensated and shown in a figure. The compensation is done around the point of the frequency curve at ca the depth 20 sample under the skin. This means that this point of the curve will stay at its original level and all points before it will be lowered and all points after it will be elevated.

The B-mode image is also displayed in a new figure where a new rectangle can be chosen. This rectangle should be placed on the temporal artery. The mean center frequency within the rectangle is calculated and displayed beside the figure. This center frequency can then be used to calculate the center frequency shift (CFS) using equation 1 and equation 2.

4. Results

4.1 Horizontalizing the skin

The four different kernels used did not give very different results after detecting the skin, removing outliers and shifting the B-mode image. The different kernels all gave ca 40 images with horizontalized skin out of 67 images in total. The first frame of all patients was used.

In some cases the skin was not horizontalized because the outliers were not removed sufficiently. See list of patients this applies to in Table 1.

2, 5
15
27
32, 36, 37, 38
43, 49
50, 51, 52, 58, 59
65, 68
70, 72, 73, 74, 78, 79
81, 82, 83, 87

Table 1. Patients where the outliers were not sufficiently removed and as a result the skin was not horizontalized properly.

Examples of original B-mode images compared with shifted B-mode images are given in Figure 13. These are not intended to represent all images, but rather to give a visual example of how the matrix changes.

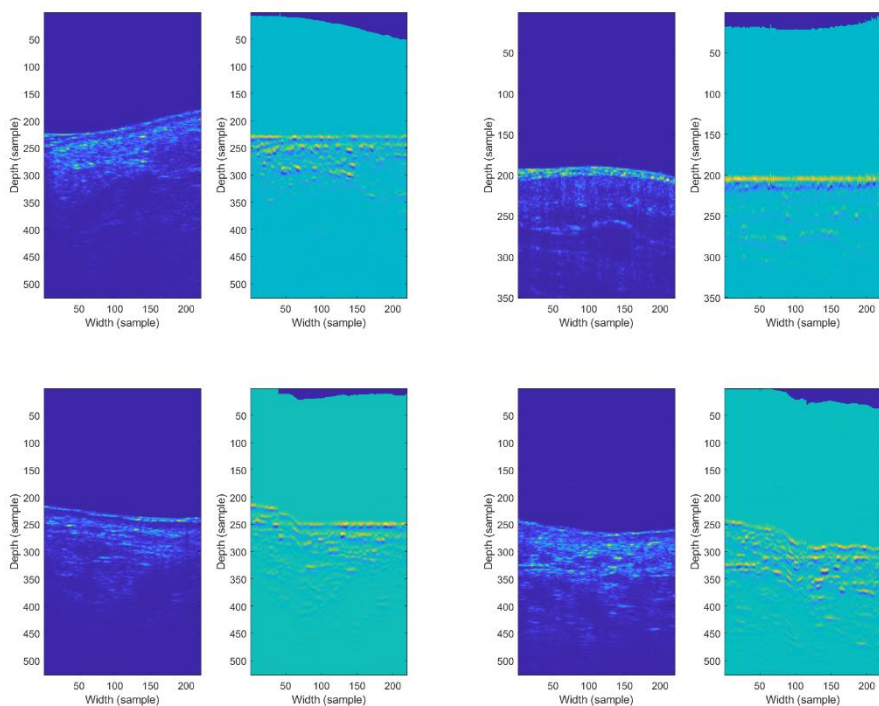


Figure 13. Top two images show cases where the shifting of the matrices was a success (left: patient 7, right: patient 9) and bottom two images show cases where the shifting of the matrices failed (left: patient 32, right: patient 74). The skin was identified using kernel1 in all images. The original image is to the left and shifted image is to the right.

There were also some B-mode images which had an appearance that differed from the majority. These matrices were difficult to shift, see Figure 14. In both these cases the horizontal line in the original image is the plastic wrap and the line with the strong curvature is the skin. The dark region between the plastic wrap and the skin is gel.

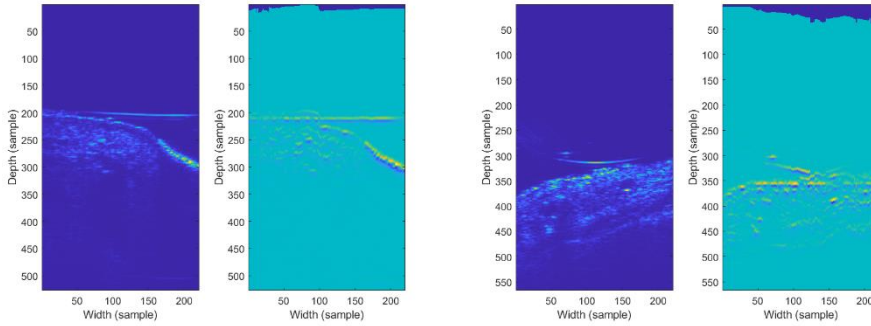


Figure 14. Two B-mode images that does not display the typical appearance and the shifted B-mode images (left: patient 51, right: patient 78). The skin was identified using kernel1 in both images. The original image is to the left and the shifted to the right.

The patients where the horizontalization of the skin was successful are listed in Table 2. The patients where the skin did not become horizontal will be excluded from calculations.

1, 3, 4, 7, 8, 9
10, 12, 13, 14
24, 25
35, 39
40, 41, 42, 44, 45, 47, 48
53, 56, 57
60, 61, 62, 63, 64, 69
71, 75, 76, 77
84, 85, 86, 88, 89
90

Table 2. List of patients where the shifting of the matrix resulted in horizontal skin.

4.2 Shifting the frequency matrix

To study the general appearance of the frequency attenuation in the tissue the frequency data was plotted for each patient, see Figure 15. Only patients where the skin was successfully horizontalized are included. Two of the patients' frequency curves did have an appearance that deviated from the typical appearance and were therefore judged to be outliers and excluded from further analysis. These were patient 1 and patient 24.

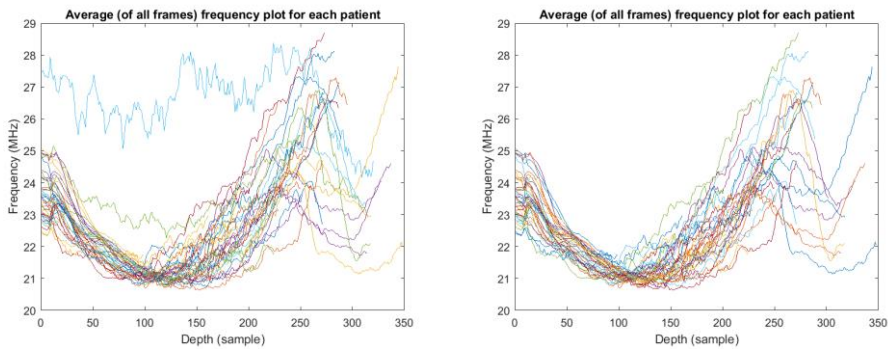


Figure 15. Left: Frequency plots for all patients where the skin was successfully horizontalized. Right: Same frequency plots, but patients 1 and 24 are also removed.

An average was made of the remaining patients frequency data, see Figure 16.

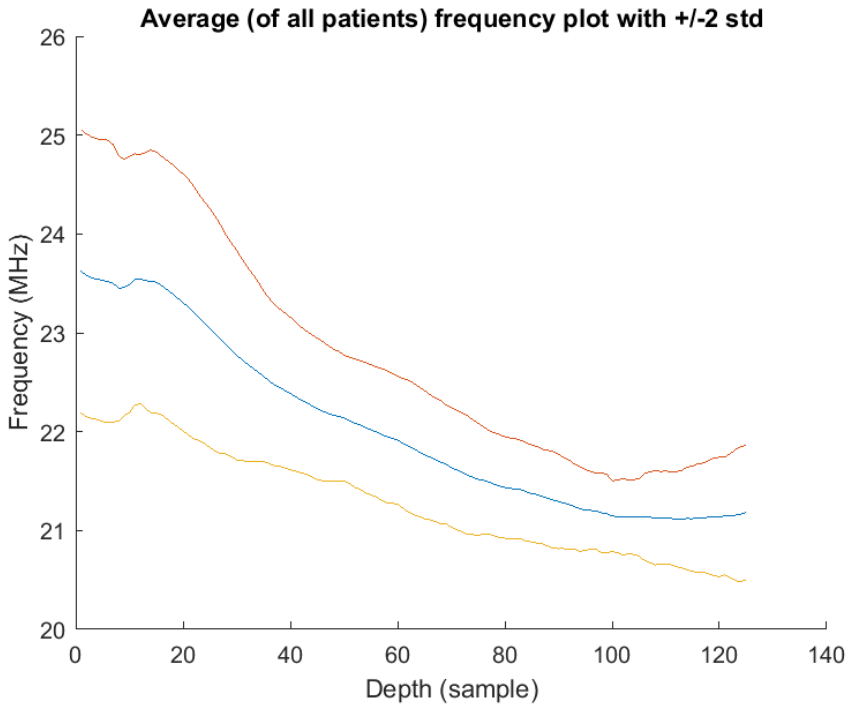


Figure 16. Average frequency plot for all patients in Table 2, except patients 1 and 24, with ± 2 standard deviations.

4.3 Measurements on phantoms

Figure 17 shows the frequency plot for the commercial phantom. Two measurements were done on the commercial phantom. The plot shows two curves, one curve for each measurement on the phantom. The curves are the average of all the frames taken during that measurement.

Figure 18 and Figure 19 show the same plot for the F16 μ m-phantom and the F49 μ m-phantom, respectively.

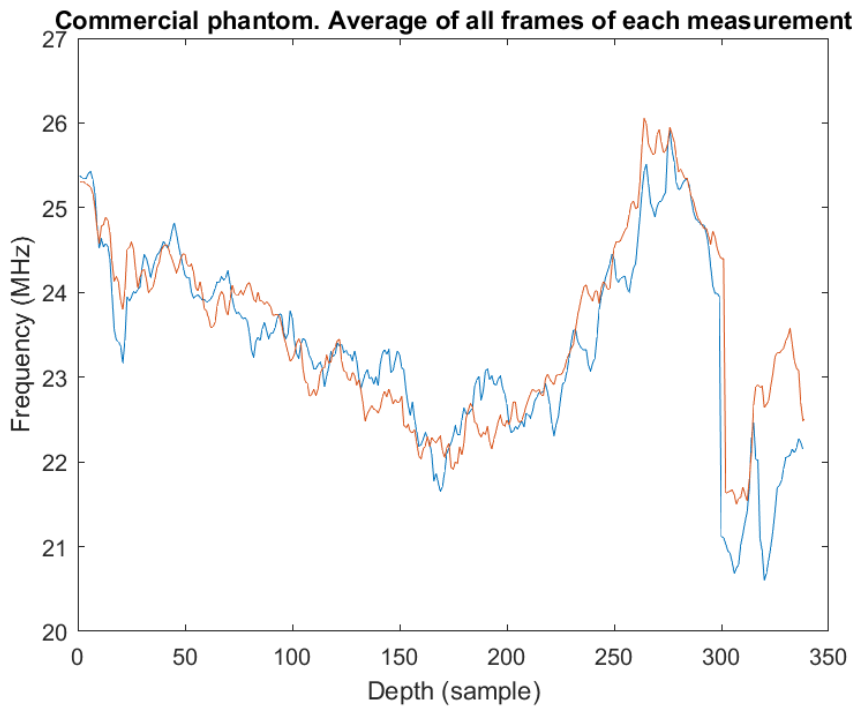


Figure 17. Frequency plot for the measurements on the commercial phantom. Average of all frames for each of the two measurements.

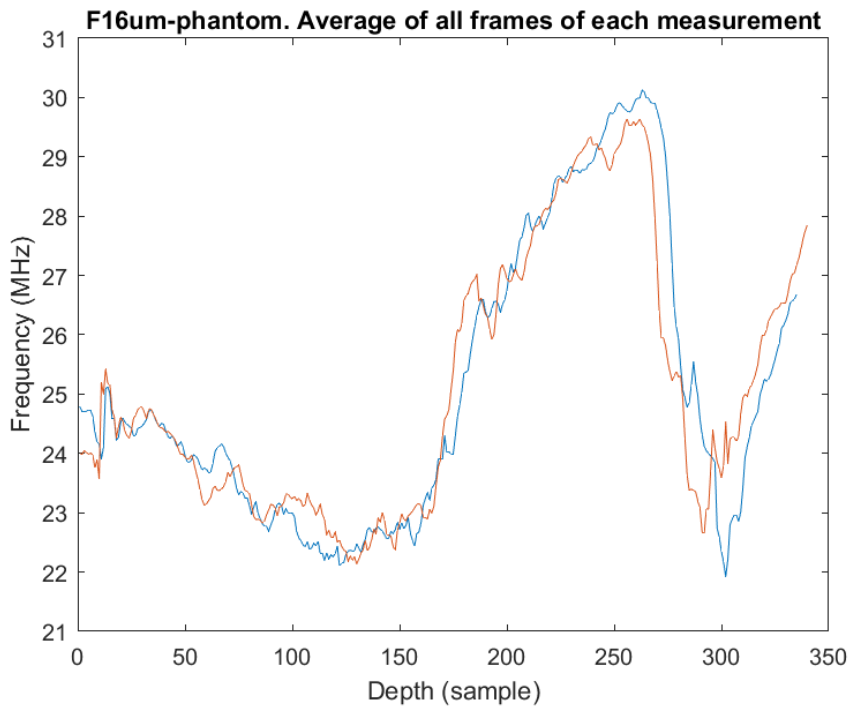


Figure 18. Frequency plot for the measurements on the F16 μ m-phantoms. Average of all frames for each of the two measurements.

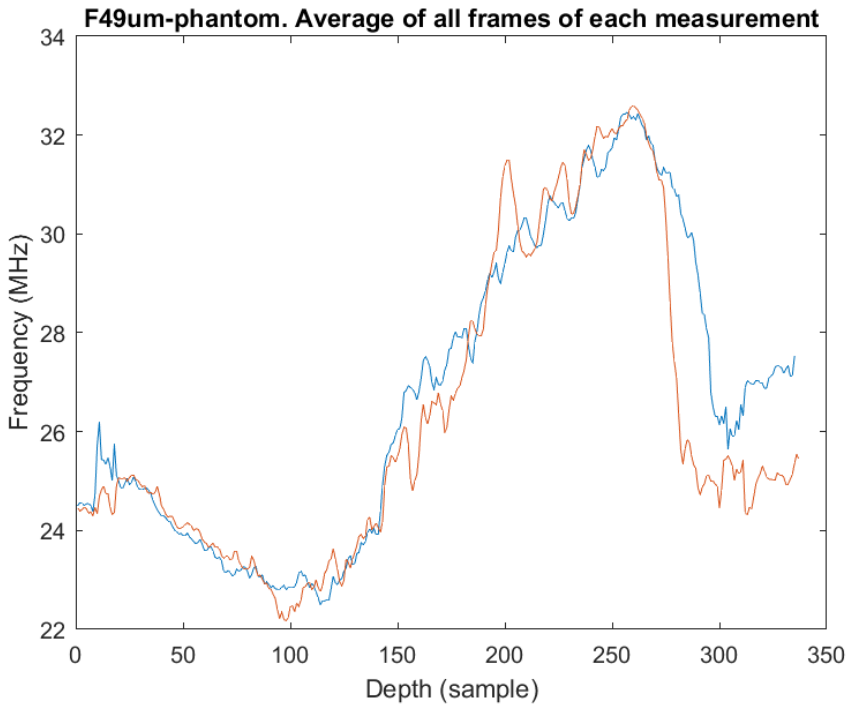


Figure 19. Frequency plot for the measurements on the F49µm-phantoms. Left: Average of all frames for each of the two measurements.

4.4 Calculating the attenuation

Figure 20 shows the linear regression modelling the frequency attenuation for each patient in the tissue between the skin and the artery. The linear regression was calculated with data between the depth of 20 and 85 samples below the skin. See average slope and standard deviation in Table 3.

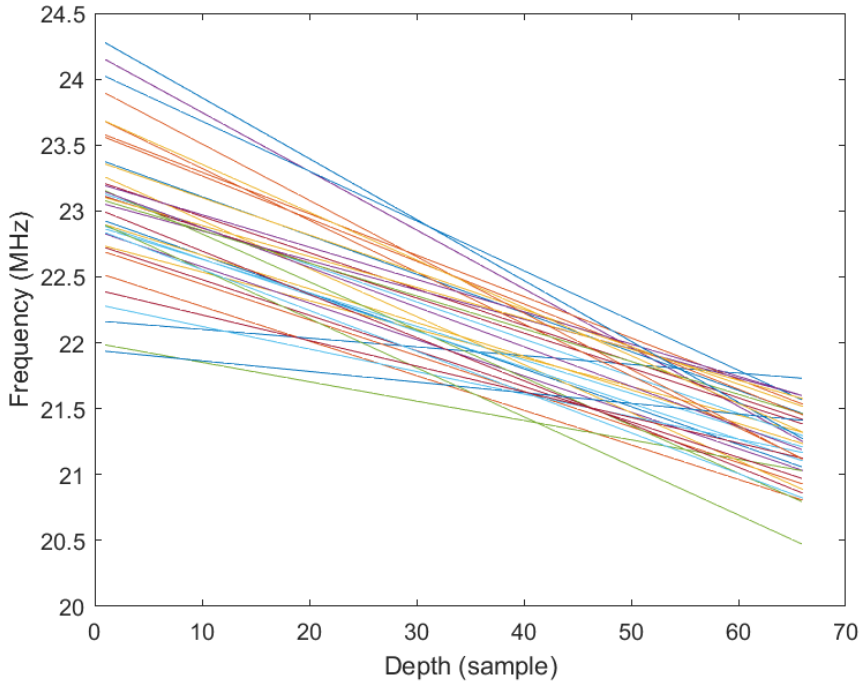


Figure 20. Linear regression modelling the frequency attenuation for each patient in the tissue calculated between the depth 20 and 85 samples below the skin. Patients where the shifting of the matrix did not result in horizontal skin are excluded, see Table 2, as well as patients 1 and 24 who had untypical frequency plots.

Average slope (k)	-0.0073
Standard deviation	0.0022

Table 3. Average slope of the linear regressions in Figure 20 and standard deviation of the slopes.

5. Discussion

5.1 Horizontalizing the skin

The attempts to find the skin and horizontalize it proved to not be fully successful. This was in most cases because the outliers were not successfully removed and in some rare cases because the skin itself was misplaced.

The main reason that the outliers were not correctly removed was that there were too many outliers when the skin had quite a strong curvature. That results in small intervals of skin that are too far apart and when one is compared to the previous the strong curvature has resulted in a too radical change in index, leading the program to misdiagnose the current skin interval as outlier.

Another reason is that there are too many outliers and too much variation between skin and outliers and no long smooth interval for the program to correctly identify as skin. In a few cases the longest interval might also be one of outliers, which result in all removal of outliers to be wrong from the start.

The skin could also be misplaced from the start when there is a lot of brighter spots below the skin, while the skin has lower intensity, which leads to skin being misplaced in the image.

There are also a few cases where the B-mode images do not have a typical appearance, see examples in Figure 14. The kernel used to identify the skin is chosen to create a maximum value of each column where the skin is. It is chosen to be used on a typical image being an image with a large low intensity field at the top followed by a high intensity field and then a noisy field at the bottom. When this is not the case, the skin might be misidentified.

Sometimes outliers were not removed because they differed too little from the surroundings for the program to consider them outliers despite that they could easily be manually identified. When determining whether two adjacent indices along the identified skin curve differ too much from each

other the difference between them are calculated and compared to a cut off value. The cut off value was chosen to identify skin and outliers as well as possible, but sometimes indices along the skin were put into the wrong category. This did however not impact the horizontalization since these outliers did not differ very much from the skin.

Due to the horizontalization of the skin not being satisfactory the decision was made to make it possible to manually interact with the B-mode image and choose in which area to calculate the attenuation. It would also prove no difficulty to manually recognize where the tissue starts after the gelpad.

However, it would be beneficial in future work to continue to improve this automatic identification of the skin since more images are continuously being added in the research. Manual identification of the skin will be cumbersome in the long run.

5.2 Measurements on phantoms

The frequency plot in Figure 16 is the average between all patients. In this plot a bump can be seen at the depth 50-60 sample. This bump could be caused by the tissue or by the ultrasound beam profile created by the transducer. If the latter is true, this bump should be compensated for in the CFS measurements. Otherwise, if it relates to the tissue, it should not be removed. The measurements on phantoms were used to investigate this.

The frequency plots from the measurements on the phantoms in Figure 17, Figure 18 and Figure 19 does not display the same bump that is visible in the *in vivo* measurements. Hence the bump is determined to be a characteristic of the tissue and not because of the ultrasound transducer. Therefore, it should not be compensated for as a part of the attenuation compensation. Judging from the frequency curves it was determined that the frequency attenuation can be assumed to be linear.

In Figure 16 the curve has a horizontal part at depth 0-20 sample. The reason behind this is uncertain and the measurements on the phantoms did not give enough information to draw any conclusion about whether the horizontal

part is due to the ultrasound transducer, the tissue or the data processing and this is a subject for further research. When calculating the slope used to compensate for the attenuation, the first horizontal part of the curve is not included in the calculations. The compensation is then done around the point to the right of the horizontal part of the curve at ca the depth 20 sample. This means that this point will stay at its original level and all points before it will be lowered and all points after it will be elevated. An alternative could be to do the compensation around the point to the left of the horizontal part of the curve. Further research is also needed to determine which is the best alternative.

5.3 Calculating the frequency attenuation

To determine whether an average attenuation value could be used to compensate for the frequency attenuation in all patients, the images where the horizontalization of the skin was successful were used. A linear regression was calculated for each patients frequency curve in using the data between the depth of 20 and 85 samples below the skin, see Figure 20. Table 3 shows the average and the standard deviation of the slopes of these linear regressions. The slopes vary quit a lot, so it was concluded that it is not possible to use a standardized slope for all patients, since this would overshadow the offset correlated to the tissue particle size that is being measured. Therefore, a feature was implemented in the GUI that calculates the attenuation for each patient individually.

6. Conclusion

Giant cell arteritis can cause serious consequences such as blindness and stroke. The available diagnostic method today is surgically removing part of an artery. Being able to investigate the artery with ultrasound is non-invasive and would be beneficial for the patient as well as being more time efficient and cost effective.

It is hypothesized that the effective particle size is different for different kinds of tissue, and therefore the ultrasound is scattered differently for diseased and health tissue. The center frequency shift of the ultrasound pulse will be used to calculate the effective particle size.

When using this method in *in vivo* studies there is always some additional tissue between the ultrasound transducer and the artery. The frequency attenuation caused by this additional tissue must be compensated for so that it does not impact the measurements of the artery.

In this project the frequency attenuation in the tissue between the ultrasound transducer and the artery was found to be linear. The frequency attenuation varied too much between the patients, so it is not possible to use the same general frequency attenuation to compensate for the frequency attenuation in all patients. Instead, the frequency attenuation is calculated individually for all patients.

A graphical user interface has been developed within the project as a tool to be used in the *in vivo* study. The GUI includes a feature to calculate and compensate for the frequency attenuation. It also includes a feature to calculate the center frequency shift caused by the artery after compensating for the frequency attenuation caused by the tissue between the ultrasound transducer and the artery.

7. References

- [1] Erlöv, T., Cinthio, M., Edsfieldt, A., Segerstedt, S., Dias, N., Nilsson, J., Gonçalves, I., Determining carotid plaque vulnerability using ultrasound center frequency shifts, *Atherosclerosis* 246 (2016) 293-300
- [2] Arthritis Foundation, *Giant Cell Arteritis*, <https://www.arthritis.org/diseases/giant-cell-arteritis> [2021-05-31]
- [3] Mayo Clinic (2021), *Giant cell arteritis*, <https://www.mayoclinic.org/diseases-conditions/giant-cell-arteritis/symptoms-causes/syc-20372758> [2021-05-31]
- [4] Hoskins, P.R., Thrush, A., Martin, K., Whittingham, T.A., ed. (2003) *Diagnostic Ultrasound Physics and Equipment*, Greenwich Medical Media
- [5] Erlöv, T., (2015) *On the Use of Ultrasound Phase Data for Arterial Characterization*, Department of Biomedical Engineering, Lund university
- [6] M.F. Insana, R.F. Wagner, D.G. Brown, T.J. Hall, Describing small-scale structure in random-media using pulse-echo ultrasound, *J. Acoust. Soc. Am.* 87 (1990)
- [7] F.L. Lizzi, M. Greenebaum, E.J. Feleppa, M. Elbaum, D.J. Coleman, Theoretical framework for spectrum analysis in ultrasonic tissue characterization, *J. Acoust. Soc. Am.* 73 (1983) 1366e1373.
- [8] Erlöv, T., Jansson, T., Persson, H. W., Cinthio, M., *Scatterer size estimation using the center frequency assessed from ultrasound time domain data*, *The Journal of the Acoustical Society of America* 140, 2352 (2016), 10.1121/1.4964107
- [9] Gray, H., 1918, *Anatomy of the human body*
- [10] Clinical translation of a novel photoacoustic imaging system for examining the temporal artery Rafi Sheikh, Magnus Cinthio, Ulf Dahlstrand, Tobias Erlov, Magdalena Naumovska, Bjorn Hammar, Sophia Zackrisson, Tomas Jansson, Nina Reistad & Malin Malmshjo, 2019, In: IEEE

Transactions on Ultrasonics, Ferroelectrics and Frequency Control. 66, 3, p.
472-480